

CoEmoGen: Towards Semantically-Coherent and Scalable Emotional Image Content Generation

Kaishen Yuan^{1*}, Yuting Zhang^{1*}, Shang Gao¹, Yijie Zhu², Wenshuo Chen¹, Yutao Yue^{1,3†}

¹The Hong Kong University of Science and Technology (Guangzhou)

²Harbin Institute of Technology (Shenzhen)

³Institute of Deep Perception Technology, JITRI

yuankaishen01@gmail.com; yutaoyue@hkust-gz.edu.cn

Abstract

Emotional Image Content Generation (EICG) aims to generate semantically clear and emotionally faithful images based on given emotion categories, with broad application prospects. While recent text-to-image diffusion models excel at generating concrete concepts, they struggle with the complexity of abstract emotions. There have also emerged methods specifically designed for EICG, but they excessively rely on word-level attribute labels for guidance, which suffer from semantic incoherence, ambiguity, and limited scalability. To address these challenges, we propose CoEmoGen, a novel pipeline notable for its semantic coherence and high scalability. Specifically, leveraging multimodal large language models (MLLMs), we construct high-quality captions focused on emotion-triggering content for context-rich semantic guidance. Furthermore, inspired by psychological insights, we design a Hierarchical Low-Rank Adaptation (HiLoRA) module to cohesively model both polarity-shared low-level features and emotion-specific high-level semantics. Extensive experiments demonstrate CoEmoGen’s superiority in emotional faithfulness and semantic coherence from quantitative, qualitative, and user study perspectives. To intuitively showcase scalability, we curate EmoArt, a large-scale dataset of emotionally evocative artistic images, providing endless inspiration for emotion-driven artistic creation. The dataset and code are available at <https://github.com/yuankaishen2001/CoEmoGen>.

Introduction

“The artist is a receptacle for emotions that come from all over the place: from the sky, from the earth...”

—Pablo Picasso

Emotion is an innate human instinct that shapes our perceptions and reactions to the world (Minsky 2007), and to better enable artificial intelligence to understand and respond to human emotional needs, affective computing has rapidly advanced in recent years (Tao and Tan 2005), with Visual Emotion Analysis (VEA) emerging as a hot research area. VEA explores the emotional information embedded in visual stimuli and analyzes human responses, offering significant potential for real-world applications such as mental health (Wieser et al. 2012; Liu et al. 2024a) and more. As the field progresses, an intriguing question arises: Can we

*Equal contributions.

†Corresponding author.



Figure 1: Comparison of sentence-level captions and word-level attribute labels as semantic guidance, where the latter suffers from (a) lack of contextual association, (b) weak correlation to emotions, and (c) missing annotations.

reverse the VEA paradigm, shifting from emotional recognition to generating images that evoke specific emotions, thereby enabling emotionally intelligent content creation?

Owing to the remarkable advancements in diffusion models (Ho and Salimans 2022; Dhariwal and Nichol 2021; Song, Meng, and Ermon 2020; Ho, Jain, and Abbeel 2020), a large number of text-to-image models have emerged, enabling users to input prompts and control conditions to generate high-quality customized images (Zhang, Rao, and Agrawala 2023; Peebles and Xie 2023; Ruiz et al. 2023; Rombach et al. 2022; Tian et al. 2025; Gal et al. 2022). Unfortunately, although these existing models are proficient at generating *concrete* concepts (e.g., *dogs, tables, cars*), they struggle and even collapse when tasked with generating *abstract* concepts such as emotions (e.g., *contentment, awe, sadness*) (Yang, Feng, and Huang 2024). This limitation hampers the progress of emotional intelligence, highlighting the urgent need for the exploration of a model capable of generating images that evoke specific emotions.

Some attempts have sought to achieve target emotion con-



Figure 2: Emotions of the same polarity exhibit similarity in low-level features but differ in high-level fine-grained semantics.

veyance by modifying the color or style of images, but their potential is constrained by fixed image content (Liu et al. 2018; Weng et al. 2023; Peng et al. 2015). From a psychological perspective, visual emotions are strongly correlated with specific semantics (Brosch, Pourtois, and Sander 2010; Tao and Tan 2005; Yuan et al. 2024; Xing et al. 2025), making mere adjustments to low-level features ineffective in conveying the intended emotion. To bridge the gap between abstract emotions and concrete images, EmoGen (Yang, Feng, and Huang 2024) pioneered the definition of Emotional Image Content Generation (EICG) as generating semantically clear and emotionally faithful visual content based on a given emotion, and explored leveraging word-level attribute labels (*i.e.*, *objects or scenes*) from EmoSet (Yang et al. 2023) as guidance to align the constructed emotion space with the semantically rich Contrastive Language-Image Pre-training (CLIP) (Radford et al. 2021) space, making a promising step toward effective emotional image generation. Nevertheless, overly relying on attribute labels poses the following limitations: (1) Restricted to word-level and used in isolation, attribute labels lack contextual connections, which prevents them from conveying comprehensive semantics (Figure 1 (a)). (2) Some annotated attribute labels may weakly correlate with emotions, while the truly emotion-triggering elements are missing, leading to ambiguity (Figure 1 (b)). (3) Attribute labels in EmoSet are not always annotated, which significantly limits the diversity and scalability of training corpus (Figure 1 (c)). Therefore, exploring ways to overcome these limitations and achieve greater flexibility in EICG is a worthwhile direction for research.

Based on the above observations, we propose Co-EmoGen, a novel pipeline towards semantically coherent and highly scalable EICG. Specifically, we focus on sentence-level captions rather than word-level attribute labels for semantically-coherent guidance, integrating visual-emotional logic through rich context and achieving align-

ment closer to human cognition. Leveraging the powerful capabilities of multimodal large language models (MLLMs) (Li et al. 2025; Lu et al. 2024; Xing et al. 2024; Hu et al. 2025), we organize effective captions that are concise yet focused on emotion-related content for the images in EmoSet, and use CLIP space for filtering to mitigate the noise inevitably introduced by MLLM hallucinations (Bai et al. 2024). Figure 1 shows the superiority of sentence-level semantically-coherent guidance over word-level guidance, while the aforementioned standardized construction paradigm also lays the foundation for high scalability. Furthermore, inspired by the psychological observation that emotions of the same polarity (*positive or negative*) share similarities in low-level visual attributes (*e.g.*, *brightness, color*) but differ in high-level semantic features (as illustrated in Figure 2) (Yang et al. 2023), we propose a Hierarchical Low-Rank Adaptation (HiLoRA) module, which includes polarity-shared LoRAs to capture common base features within the same polarity and emotion-specific LoRAs to learn the fine-grained exclusive elements of specific emotions. Extensive experiments, including quantitative comparisons, qualitative analyses, and a user study, demonstrate the superiority of CoEmoGen in semantic coherence and emotional fidelity. To further showcase its scalability, we collect EmoArt, a dataset of 13,633 emotionally evocative artistic images, which CoEmoGen effortlessly leverages to inspire artists in creating emotion-driven artworks. Our contributions can be summarized as follows:

- We propose CoEmoGen, a novel semantically-coherent and highly scalable EICG pipeline.
- We introduce reliable captions with emotion-related content for EmoSet, leveraging their rich coherent context for sentence-level semantic guidance.
- Inspired by psychology, we design a HiLoRA module with polarity-shared LoRAs for modeling the common base features and emotion-specific LoRAs for capturing the fine-grained exclusive elements.
- Extensive experiments, encompassing quantitative, qualitative, and a user study, showcase CoEmoGen’s superiority in EICG, while EmoArt, a dataset composed of emotionally stimulating artworks, is constructed to further highlight its flexible scalability.

Related Work

Visual emotion analysis. Visual Emotion Analysis (VEA) aims to predict people’s emotional responses to visual stimuli and has been studied for over two decades (Zhao et al. 2021). The most commonly employed Mikels model classifies emotions into eight categories: *amusement, awe, contentment, excitement, anger, disgust, fear,* and *sadness*, with the first four belonging to the *positive* polarity and the latter four to the *negative* polarity (Mikels et al. 2005). In the early stages, inspired by psychology and art theory, Machajdik *et al.* (Machajdik and Hanbury 2010) extracted specific image features related to emotions, such as color and composition, for analysis. Borth *et al.* (Borth et al. 2013) constructed a Visual Sentiment Ontology (VSO) containing over 3,000 adjective-noun pairs (ANP), learning visual emotions from a semantic perspective. With the rapid develop-

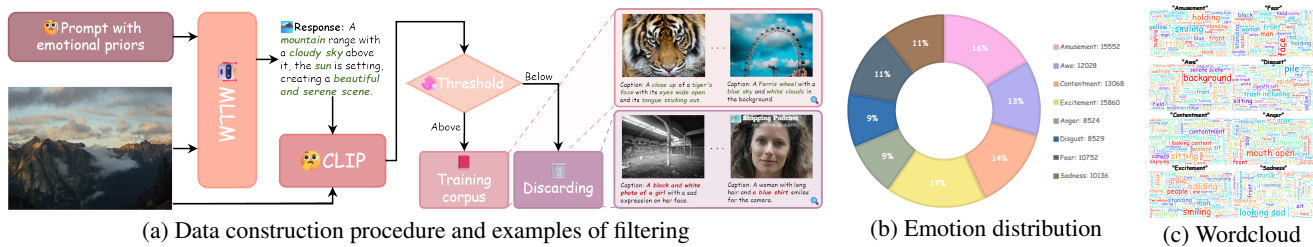


Figure 3: Summary of sentence-level coherent semantic guidance acquisition

ment of deep learning, Rao *et al.* proposed MldrNet (Rao, Li, and Xu 2020), which integrates different levels of deep representations (image semantics, aesthetics, and low-level features) to classify emotions across various types of images. Yang *et al.* (Yang et al. 2018) used object detection and attention mechanisms to capture both global and local relationships for emotion prediction. Yang *et al.* (Yang et al. 2021) first introduced stimulus selection, extracting unique emotional features from different stimuli. Ultimately, VEA is a classification task, while reversing this process to generate images that evoke specific emotions has broad practical applications in areas such as mental health and artistic creation, making it worth further exploration.

Emotional image content generation. Recently, with the remarkable progress of diffusion models (Ho and Salimans 2022; Dhariwal and Nichol 2021; Song, Meng, and Ermon 2020; Ho, Jain, and Abbeel 2020), a large number of text-to-image models have emerged, allowing users to generate high-quality and diverse images (Peebles and Xie 2023; Betker et al. 2023; Rombach et al. 2022; Tian et al. 2025; Saharia et al. 2022; Nichol et al. 2021). Furthermore, to achieve customization, several personalized text-to-image generation methods (Zhang, Rao, and Agrawala 2023; Ruiz et al. 2023; Gal et al. 2022; Zhu et al. 2024; Kim et al. 2024; Kumari et al. 2023; Chen et al. 2024, 2025) have been proposed, which typically rely on learning new embeddings or fine-tuning model parameters. While these methods have attained impressive results in generating concrete concepts, they fall short when it comes to abstract concepts such as emotions. Some attempts (Chen et al. 2020; Liu et al. 2018; Peng et al. 2015; Wang, Jia, and Cai 2013; Sun et al. 2023; Weng et al. 2023; Liu et al. 2024b; Zhang et al. 2025b) aim to modify low-level visual elements to alter the emotional tone of input image, thus performing image emotion transfer. Representative works include Peng *et al.*'s (Peng et al. 2015) changing the emotions evoked by adjusting the image's color and texture features, and Sun *et al.*'s proposal (Sun et al. 2023) to activate a specified emotion through style transfer. Due to the fixed content of the image, and the strong correlation between visual emotions and specific semantics, simply modifying these superficial features is insufficient to evoke the desired emotion. Therefore, EmoGen (Yang, Feng, and Huang 2024) initially defined the EICG task as creating semantically clear and emotionally faithful visual content based on a specified emotion category, and it achieved promising outcomes in generating emotionally evocative images. Nevertheless, due to the reliance on word-level attribute labels, which lack semantic context, are weakly related to emotions, and often suffer

from label deficiencies, EmoGen lacks semantic coherence and flexibility in practical applications. Unlike EmoGen, the proposed CoEmoGen introduces sentence-level captions as supervision and designs a HiLoRA module in accordance with psychological consensus, resulting in a semantically-coherent and highly scalable EICG pipeline that excels in both semantic clarity and emotional fidelity.

Methodology

Coherent semantic acquisition

EmoSet (Yang et al. 2023) is a recently constructed large-scale visual emotion dataset that follows the popular eight-category Mikels model (Mikels et al. 2005). It retrieves relevant images from the Internet based on emotions and their synonyms, annotating 118,102 images not only with emotional labels but also with emotion-related visual attributes at different levels, including low-level (*i.e.*, *brightness*, *colorfulness*), mid-level (*i.e.*, *scene type*, *object class*), and high-level (*i.e.*, *facial expressions*, *human actions*). The annotation process is semi-automated; for example, scene types are annotated using a scene recognition model trained on Places365 dataset (Zhou et al. 2017), while object classes are annotated using an object detection model trained on Open-ImagesV4 dataset (Kuznetsova et al. 2020). Despite manual intervention for corrections, these word-level labels still suffer from a lack of coherent associations, emotional ambiguity, and missing elements. As a result, EmoGen (Yang, Feng, and Huang 2024), which relies on attribute labels such as scenes or objects for semantic guidance, faces challenges in terms of semantic coherence and the scalability of the training corpus.

Recognizing the shortcomings of attribute label supervision, we seek to introduce context-rich and coherent sentence-level captions as guidance. Thanks to the remarkable capabilities demonstrated by recent MLLMs (Li et al. 2025; Zhang et al. 2025a,c), generating a tailored caption for an image has become cost-effective and feasible. Based on this, we meticulously design a prompt that takes the given image's corresponding emotion label as prior knowledge while enforcing a focus on different levels of emotion-related visual attributes, aligning with those mentioned in EmoSet, thereby encouraging MLLMs to produce a concise yet emotion-rich caption. The designed prompt is as follows:

<Image> This image evokes a strong emotion of <emotion>. Provide a *one-sentence caption* that vividly describes the visual details, focusing on elements like *brightness*, *colorfulness*, *scene type*, *object classes*, *facial expressions*, and *human actions* that effectively convey and express this emotion.

We investigate the impact of captions obtained from different prompts on subsequent emotional image generation,

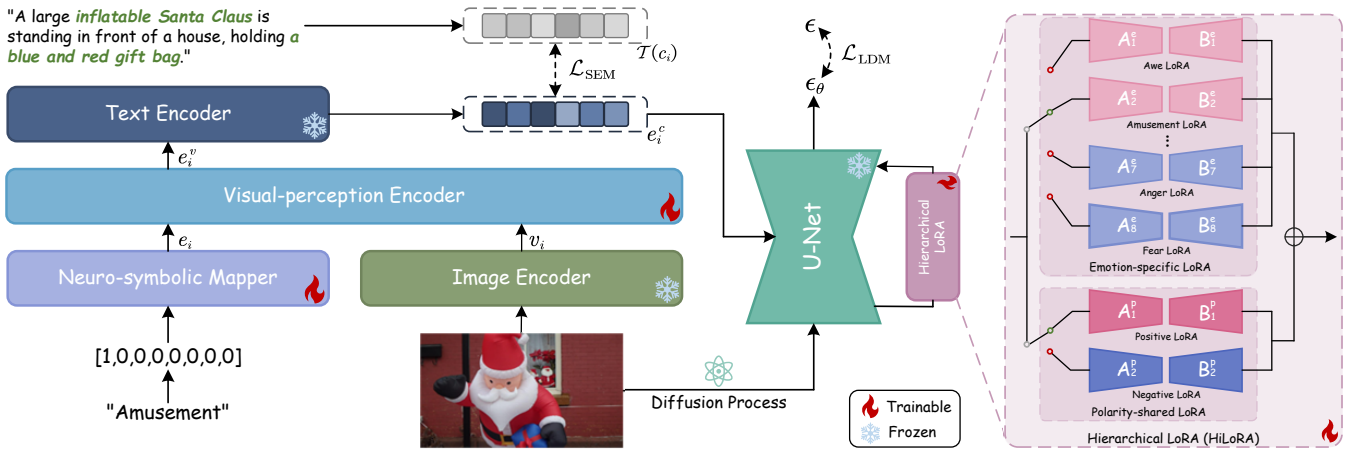


Figure 4: The overall architecture of the proposed CoEomoGen. The one-hot vectors derived from emotion categories first undergo neuro-symbolic mapping and interact with the visual embedding, then are encoded by the text encoder to obtain emotion conditions, which further guide the denoising network U-Net equipped with HiLoRA, which consists of emotion-specific LoRAs and polarity-shared LoRAs.

with details provided in the ablation studies. We equip all images in EmoSet with corresponding captions. However, it is worth noting that due to the inherent hallucinations of MLLMs, which refer to a phenomenon where models generate unrealistic or fabricated content (Bai et al. 2024), some inaccurate captions are inevitably produced. To address this, we compute the similarity of the preliminarily obtained image-caption pairs in the CLIP space (Radford et al. 2021), discarding the bottom 20% of samples in each category based on similarity rankings to ensure sufficiently reliable semantic guidance. The standardized data construction procedure sets the stage for high scalability, and this entire process, along with examples of filtering, is shown in Figure 3 (a). The emotional distribution of the final training corpus is presented in Figure 3 (b), while a word cloud for each emotion, based on corresponding captions, is shown in Figure 3 (c), with clearer ones provided in Appendix.

CoEomoGen

Based on the aforementioned constructed dataset \mathcal{D} , we propose CoEomoGen, an EICG pipeline developed for semantic coherence and high scalability.

Overview. Given a sample $\mathcal{D}_i = \{I_i, y_i, c_i\}$, where I_i represents the i -th image, y_i denotes the corresponding emotion label, and c_i indicates the generated caption, we first apply one-hot encoding to y_i , setting the position of the present category to 1 and all others to 0, obtaining y_i^o . The input y_i^o is then processed by a Neuro-symbolic Mapper composed of fully connected layers with non-linear activations to obtain the emotional descriptor e_i . This neuro-symbolic mapping provides greater flexibility and diversity in emotional image generation, which is further discussed in the ablation studies. To achieve more precise alignment with contextually coherent and semantically rich captions, enhancing perception and interaction with visual information is beneficial. Specifically, we fuse the neuro-symbolic vector e_i with the visual embedding v_i , which is obtained by encoding I_i through the CLIP image encoder, utilizing a Visual-Perception Encoder primarily based on a cross-attention mechanism. This pro-

cess can be formulated as follows:

$$e_i^v = \text{Softmax}\left(\frac{e_i W_q (v_i W_k)^T}{\sqrt{d_0}}\right) v_i W_v, \quad (1)$$

where e_i^v is visually-enhanced emotion descriptor, W_q , W_k , and W_v are learnable weights, and d_0 is feature dimension. Subsequently, e_i^v is fed into CLIP text encoder to obtain the emotion condition e_i^c , which further contributes to the U-Net equipped with Hierarchical LoRA. The entire process described above is illustrated on the left side of Figure 4.

Hierarchical LoRA. Low-Rank Adaptation (LoRA) (Hu et al. 2022) is a popular parameter-efficient fine-tuning technique that trains only a small number of parameters through low-rank matrix decomposition, enabling the fine-tuning of pre-trained model weights at a lower computational cost. Its core concept can be formulated as follows:

$$W' = W + \Delta W = W + A \cdot B, \Delta W = A \cdot B \quad (2)$$

where W and $W' \in \mathbb{R}^{d \times d'}$ represent the weights before and after adaptation, respectively, with $A \in \mathbb{R}^{d \times r}$ and $B \in \mathbb{R}^{r \times d'}$ being the introduced low-rank adaptation matrices, satisfying the condition $r \ll \min(d, d')$.

However, in performing EICG, when dealing with the complex concept of representing emotions, a single LoRA proves insufficient. Inspired by psychological observations that emotions with the same polarity share common characteristics in low-level features such as brightness while differing in high-level semantic elements (as shown in Figure 2), we design a hierarchical LoRA (HiLoRA) module, which consists of eight emotion-specific LoRAs $\{\Delta W_j^e\}_{j=1}^8$ tailored to each emotion and two polarity-shared LoRAs $\{\Delta W_k^p\}_{k=1}^2$. These LoRAs function with distinct roles, with only the LoRAs corresponding to the input image’s emotion label and its associated polarity activated during updates. Taking *amusement* ($j = 2$) under the *positive* polarity ($k = 1$) as an example, Equation 2 transforms into:

$$W' = W + \Delta W_1^p + \Delta W_2^e = W + A_1^p \cdot B_1^p + A_2^e \cdot B_2^e. \quad (3)$$

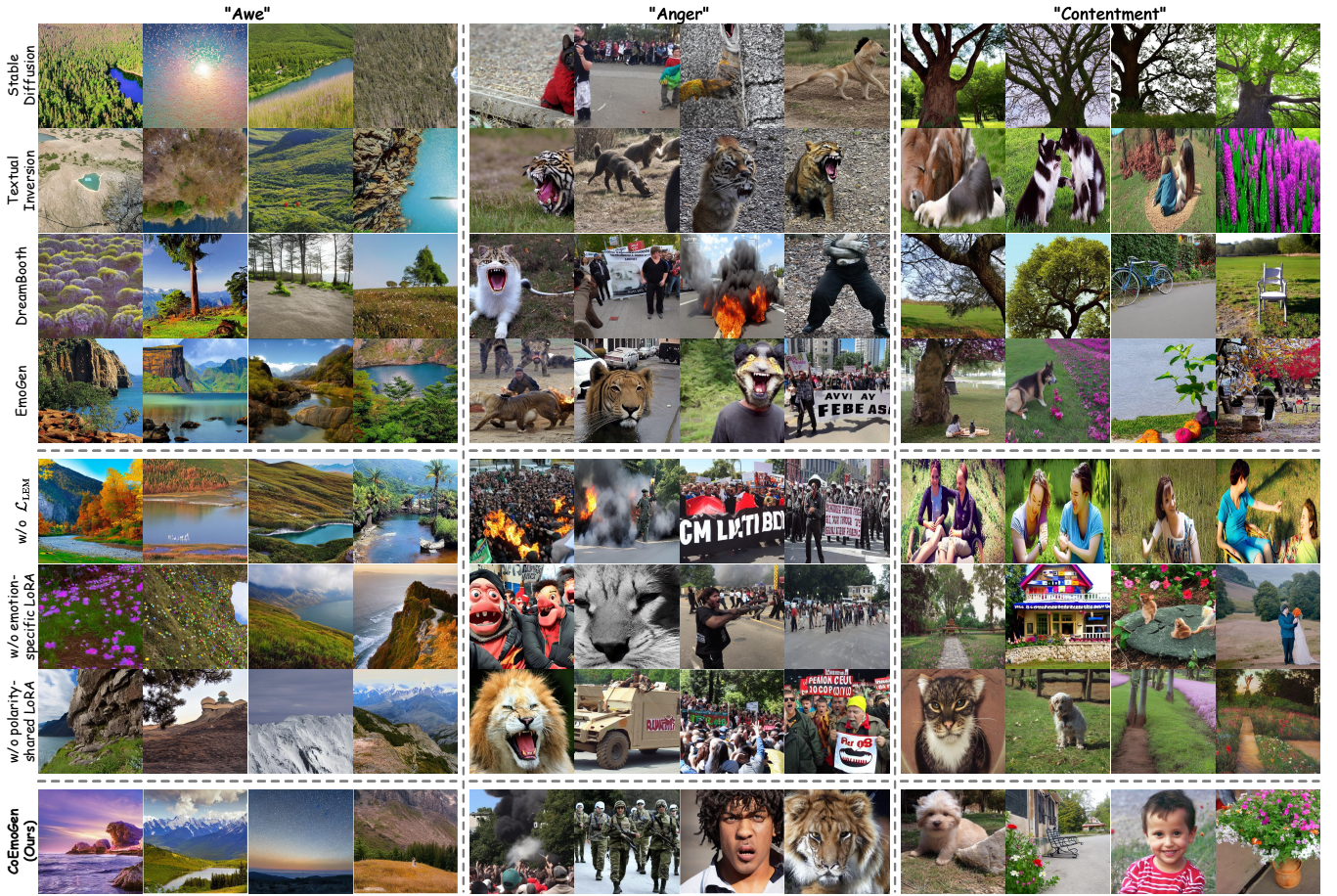


Figure 5: Qualitative comparisons of the proposed CoEmoGen with state-of-the-art generation methods and ablation variants.

Here, ΔW_1^p is responsible for modeling the high brightness and colorfulness associated with the *positive* polarity, while ΔW_2^e captures the high-level fine-grained semantics related to *amusement*. The detailed structure of HiLoRA is shown on the right side of Figure 4.

Loss function. During training, we optimize the Neuro-symbolic Mapper, Visual-perception Encoder, and HiLoRA while keeping the image encoder, text encoder, and U-Net frozen. Our loss constraints consist of two components. One is the Latent Diffusion Model (LDM) loss (Rombach et al. 2022), which guides the learning of pixel-level representations:

$$\mathcal{L}_{\text{LDM}} = \mathbb{E}_{\mathcal{E}(\cdot), I_i, e_i^c, \epsilon, t} \left[\|\epsilon - \epsilon_\theta(z_t, t, \mathcal{E}(I_i), e_i^c)\|_2^2 \right], \quad (4)$$

where $\mathcal{E}(\cdot)$ denotes the latent encoder, $\epsilon_\theta(\cdot)$ indicates the denoising network U-Net, ϵ refers to the added noise, and z_t is the latent noise at time step t . However, applying \mathcal{L}_{LDM} alone may lead to an excessive focus on pixel-level commonalities and even collapse into specific semantics. To maintain the semantic diversity and coherence of the same emotion, we explicitly approximate the cosine similarity between the emotion condition e_i^c and the encoded sentence-level caption in the CLIP space, introducing the semantic loss \mathcal{L}_{SEM} , formulated as follows:

$$\mathcal{L}_{\text{SEM}} = 1 - \frac{e_i^c \cdot \mathcal{T}(c_i)}{\|e_i^c\| \|\mathcal{T}(c_i)\|}, \quad (5)$$

where \mathcal{T} is the CLIP text encoder. The combination of the above two losses achieves synergy between pixel-level guidance and sentence-level coherent semantic guidance.

During inference, similar to EmoGen (Yang, Feng, and Huang 2024), we obtain visual embedding v_i by randomly sampling from corresponding emotion cluster, which is pre-constructed and represented by a Gaussian distribution, achieving a high degree of diversity.

Experiments

Settings

Implementation details. We initialize the latent encoder and denoising network with pre-trained weights from Stable Diffusion v1.5 (Rombach et al. 2022) and choose the pre-trained CLIP ViT-L/14 (Radford et al. 2021) model for both the image and text encoders to ensure a fair comparison. Regarding the model configuration, the hidden layer size of the Neuro-symbolic Mapper is set to 512, the embedding dimension d_0 in the Visual-perception Encoder is set to 768, and the rank r in HiLoRA is set to 4. During training, we set the batch size to 1, utilize the AdamW (Loshchilov and Hutter 2017) optimizer with $\beta_1 = 0.9$, $\beta_2 = 0.999$, a weight decay of $1e^{-2}$, and a constant learning rate of $1e^{-3}$ for 130,000 iterations. Following EmoGen (Yang, Feng, and Huang 2024), we also adopt a random oversampling

Table 1: Quantitative comparisons with state-of-the-art methods and ablation variants on the EICG task, covering five metrics.

Method	FID↓	LPIPS↑	Emo-A↑	Sem-C↑	Sem-D↑
Stable Diffusion (Rombach et al. 2022)	44.05	0.687	70.77%	0.608	0.0199
Textual Inversion (Gal et al. 2022)	50.51	0.702	74.87%	0.605	0.0282
DreamBooth (Ruiz et al. 2023)	46.89	0.661	70.50%	0.614	0.0178
EmoGen (Yang, Feng, and Huang 2024)	41.60	0.717	76.25%	0.633	0.0335
CoEmoGen (Ours)	40.66	0.732	80.15%	0.641	0.0349
w/o \mathcal{L}_{SEM}	50.32	0.698	65.90%	0.562	0.0255
w/o emotion-specific LoRAs	45.30	0.713	75.37%	0.625	0.0308
w/o polarity-shared LoRAs	41.47	0.724	78.83%	0.638	0.0336

strategy to help mitigate class imbalance. All experiments are conducted on two NVIDIA RTX 4090 GPUs with PyTorch (Paszke et al. 2019).

Metrics. To comprehensively evaluate model’s performance in executing the EICG task in terms of emotion fidelity, semantic clarity, and semantic diversity, following EmoGen (Yang, Feng, and Huang 2024), we generate 1,000 images for each emotion and employ five evaluation metrics: (1) **FID** (Heusel et al. 2017) to measure the distribution distance between generated and real images to assess fidelity, (2) **LPIPS** (Zhang et al. 2018) to assess the overall diversity of the generated images, (3) **Emo-A** (Emotion Accuracy) based on emotion classification accuracy to evaluate the consistency between the generated images and the target emotion, (4) **Sem-C** (Semantic Clarity) to measure the explicitness of the generated image contents, and (5) **Sem-D** (Semantic Diversity) to quantify the richness of content corresponding to each emotion in the generated images. The implementation details of these metrics are in the Appendix.

Comparisons

We compare the proposed CoEmoGen with the most relevant and state-of-the-art generation models, including the general image generation model Stable Diffusion (Rombach et al. 2022), the customized image generation models Textual Inversion (Gal et al. 2022) and Dreambooth (Ruiz et al. 2023), as well as EmoGen (Yang, Feng, and Huang 2024), which is specifically designed for EICG. The fine-tuning of all the above comparison methods is consistent with that in EmoGen.

Qualitative analysis. Figure 5 presents a qualitative comparison between our proposed CoEmoGen and state-of-the-art methods, with analysis focused on three emotional categories: *awe*, *anger*, and *contentment* (complete results for all emotions are provided in the Appendix). It can be observed that both general and customized image generation models struggle to capture the complex and diverse semantic elements of a specific emotion, often collapsing into a single feature point or exhibiting severe semantic distortion, which makes them highly uncontrollable. In comparison, EmoGen introduces attribute labels as semantic guidance, improving diversity and emotional conveyance, whereas, constrained by the word-level supervision, it unintentionally binds emotions to specific objects or scenes, leading to unnatural collage-like combinations that challenge semantic coherence. For example, *anger* is frequently associated with *fire*, *tigers*, and *wide-open mouths*, and although EmoGen

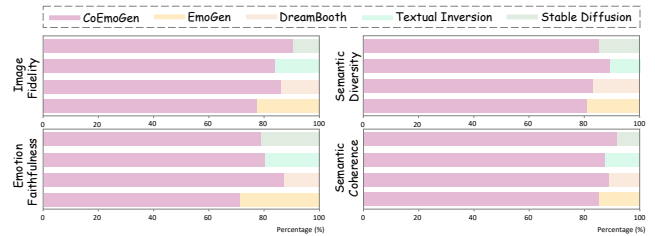


Figure 6: User study results on preference selection between CoEmoGen and a comparative method regarding image fidelity, emotion faithfulness, semantic diversity, and semantic coherence.

indeed successfully captures these elements, it fails to consider their semantic relationships, resulting in unrealistic outputs such as a *flaming tiger*. In contrast, the proposed CoEmoGen achieves more natural and vivid emotion conveyance, owing to context-rich sentence-level captions that constrain logical connections between elements as guidance, which ensures semantic coherence. Moreover, CoEmoGen preserves diversity while generating images with richer colors and smoother visuals, drawing from the cooperation of emotion-specific LoRAs for fine-grained semantics capture and polarity-shared LoRAs for low-level feature modeling in HiLoRA. Another noteworthy aspect is that CoEmoGen demonstrates versatile photographic composition, rooted in camera-related words like “close-up” in the captions, giving the generated images a stronger sense of perspective and realism.

Quantitative comparison. Table 1 quantitatively compares CoEmoGen with other methods, demonstrating its overall performance advantage by leading across all five evaluation metrics. Specifically, Emo-A shows an improvement of at least 3.9%, confirming the accuracy of emotional conveyance in the generated images. FID indicates that the generated images better align with the real data distribution, while Sem-C ensures consistent semantic clarity throughout the generation process. Additionally, LPIPS and Sem-D highlight the dual advantages of visual diversity and semantic richness in the generated results. These quantitative findings align with the visualizations in Figure 5, jointly proving CoEmoGen’s superiority in achieving the EICG task.

User study. To evaluate whether CoEmoGen’s generation aligns with human perceptual cognition, we further conduct a comprehensive user study in addition to the aforementioned qualitative and quantitative analyses. The user study involved 17 participants (8 female and 9 male) aged 13-51 with diverse backgrounds. Each participant was presented with two image groups conveying the same target emotions, one generated by CoEmoGen and the other by a comparative method, and asked to select their preference through four criteria-oriented questions: (1) “Which group appears more realistic?” (*Image fidelity*); (2) “Which group better evokes [specific emotion]?” (*Emotion faithfulness*); (3) “Which group shows greater diversity?” (*Semantic diversity*); (4) “Which group demonstrates more natural coherence?” (*Semantic coherence*). As evidenced in Figure 6, CoEmoGen achieves overwhelming preference across all four dimensions, particularly excelling in semantic coher-

ence with an average selection rate of 88.42%. Notably, despite being relatively close to EmoGen in some quantitative metrics, CoEmoGen secures an average user preference rate of 78.67% in direct pairwise comparisons, demonstrating superior alignment with human emotional perception and cognitive intuition, which ultimately translates into stronger emotional resonance in practical applications.

Ablation Study

We conduct ablation studies to explore the effects of each component of the proposed CoEmoGen, as well as the selection of important settings.

We individually remove each component from the complete CoEmoGen and observe the results to explore its effect, which is quantitatively presented in Table 1 and qualitatively shown in Figure 5. **Semantic loss.** It can be observed that when \mathcal{L}_{SEM} is absent, the model, deprived of the essential semantic guidance and relying solely on \mathcal{L}_{LDM} , excessively focuses on pixel-level reconstruction, even collapsing into specific semantics, leading to significant semantic distortion and a lack of semantic diversity. **Emotion-specific LoRAs.** When emotion-specific LoRAs are removed, the model’s ability to capture emotion-specific fine-grained semantics diminishes. Meanwhile, the effect of polarity-shared LoRAs introduces semantic entanglement among emotions belonging to the same polarity. As a result, although the model performs reasonably well in terms of semantic clarity and diversity, the semantic confusion among emotions of the same polarity significantly reduces the accuracy of conveying the target emotion and amplifies the divergence from the true distribution. **Polarity-shared LoRAs.** In comparison, when polarity-shared LoRAs are removed, the quantitative results appear to show only a slight decline compared to the complete CoEmoGen. However, qualitative comparisons reveal that the color saturation and brightness tend to become overly monotonous or unnatural, which further confirms the important role of polarity-shared LoRAs in modeling the low-level features of polarity. In summary, each component of CoEmoGen performs its specific function, and when working in unison, they exhibit the optimal performance in terms of emotional fidelity, semantic diversity and coherence.

Table 2 compares the results of different choices of important settings. **Type of caption.** To obtain the most suitable captions as sentence-level semantic guidance, we explore four prompts to drive the MLLMs, controlling whether the captions focus on emotion-related elements and contain complete details, with further details provided in the Appendix. As shown in Table 2 (a), adding emotional priors to the prompt promotes consistent improvement in the model’s ability, highlighting the importance of focusing on emotional elements. However, removing the restriction to generate only one sentence and allowing the inclusion of as many details as possible leads to performance degradation, likely due to the noise introduced by irrelevant elements and the increased risk of hallucinations in MLLMs with longer captions, making model convergence more difficult. Therefore, we ultimately choose a prompt with emotional priors and the constraint of generating a single sentence. **Type of**

Emotional Prior	Details	FID↓	LPIPS↑	Emo-A↑	Sem-C↑	Sem-D↑
\times	\times	43.32	0.714	75.29%	0.612	0.0303
✓	\times	40.66	0.732	80.15%	0.641	0.0349
\times	✓	44.91	0.716	73.68%	0.604	0.0315
✓	✓	42.58	0.724	77.42%	0.628	0.0338

(a) Type of captions for semantic guidance.

Type of Input	FID↓	LPIPS↑	Emo-A↑	Sem-C↑	Sem-D↑
Learnable	43.77	0.705	78.49%	0.593	0.0289
Text	42.38	0.697	78.92%	0.611	0.0275
One-hot	40.66	0.732	80.15%	0.641	0.0349

(b) Type of inputs for emotion representation.

Type of \mathcal{L}_{SEM}	FID↓	LPIPS↑	Emo-A↑	Sem-C↑	Sem-D↑
MAE	42.40	0.721	78.83%	0.626	0.0311
MSE	41.87	0.725	79.04%	0.618	0.0327
K-L	48.36	0.693	70.01%	0.609	0.0272
Cosine	40.66	0.732	80.15%	0.641	0.0349

(c) Type of semantic constraint mechanisms in \mathcal{L}_{SEM} .

Table 2: Quantitative results of CoEmoGen with different choices of important settings. Default settings are in **gray**.

input. We compare three different types of input representations, including learnable class vectors, frozen text encodings of emotion class names, and the one-hot vectors with the Neuro-symbolic Mapper. As shown in Table 2 (b), experimental results reveal significant limitations in the first two types in terms of diversity, which is due to the representation bottleneck from the limited capacity of learnable vectors and over-constraining semantics in the embedding space from the frozen text encoder. In contrast, the Neuro-symbolic Mapper expands the latent space exploration while maintaining semantic consistency through a differentiable symbolic reasoning mechanism, enabling greater diversity. **Design of \mathcal{L}_{SEM} .** In the design of the semantic loss \mathcal{L}_{SEM} , constructing an effective semantic constraint mechanism is a question worth considering. To address this, we systematically compare the performance differences of four constraint methods: Mean Absolute Error (MAE), Mean Squared Error (MSE), Kullback-Leibler Divergence (K-L divergence), and Cosine Similarity. As shown in Table 2 (c), Cosine Similarity achieves the best performance, owing to its inherent advantage in measuring semantic similarity in high-dimensional vector spaces, enabling more precise guidance for the model to capture deep semantic relationships. Therefore, we choose it by default.

Scalability of CoEmoGen

Thanks to MLLMs facilitating the accessibility of sentence-level semantic guidance captions, CoEmoGen exhibits high scalability compared to EmoGen, which relies on high acquisition costs and limited word-level attribute labels for supervision. This feature enables CoEmoGen to incorporate any emotionally evocative images into the training corpus.

To illustrate this, we construct the first large-scale emotional art image dataset, **EmoArt**. Specifically, we first collect approximately 100,000 artistic images from WikiArt, covering 129 artists, 11 genres, and 27 styles. Then, we uti-



Figure 7: Visualization of emotionally evocative artistic images generated by EmoArt-driven CoEmoGen.

lize a classifier pre-trained on EmoSet to predict the emotional categories of these artistic images, setting an emotion confidence threshold of 0.75, which ultimately filters out 13,633 strongly emotion-representative samples. Notably, due to the low-frequency presence of *excitement* and *disgust* in artistic expressions (accounting for less than 1%) (Pearce et al. 2016), EmoArt focuses on the remaining six emotion categories. A visualization of EmoArt’s images across different emotions is provided in Appendix. Next, following the same process as Figure 3 (a), we obtain reliable sentence-level captions for each image, which are then utilized to train CoEmoGen. Figure 7 presents the results generated by EmoArt-driven CoEmoGen, demonstrating its ability to create emotionally faithful and stylistically diverse artistic images for each emotion category, offering endless inspiration for artists in crafting emotionally evocative artworks.

The construction of EmoArt intuitively showcases CoEmoGen’s high flexibility and scalability, allowing users to follow a standardized construction paradigm to effortlessly customize diverse emotion-rich datasets and generate emotionally stimulating images tailored to their specific needs.

Applications

Given its strong emotional content generation capability, we further explore CoEmoGen’s intriguing applications. **Emotion Transfer.** By integrating the emotional representations learned by CoEmoGen with common neutral elements, we achieve targeted emotion transfer, as shown in Figure 8. Excitingly, this results in a seamless fusion, where the emotional semantics are incorporated while staying true to the original neutral elements. Importantly, instead of rigidly overlaying emotion-related elements onto the neutral ones, this process perceives the semantic characteristics of the neutral elements and adaptively adjusts their textures, colors, and layouts to ensure overall coherence. For example, in the fear transfer applied to a street scene, CoEmoGen enhances shadow contrast and spatial depth, generating a dark and deep corridor that aligns with real-world lighting principles rather than mechanically adding horror symbols, ensuring a gradual and immersive infusion of emotional semantics and



Figure 8: Visualization of emotion transfer by fusing emotion representations with neutral elements.



Figure 9: Visualization of emotion fusion by combining different emotion representations.

offering promising potential for interpretable image emotional editing. **Emotion Fusion.** We also explore the possibility of combining different emotional representations, as shown in Figure 9, which illustrates the pairwise combinations of *amusement*, *awe*, and *fear*, showcasing a visually rich narrative intertwined with complex emotions. For example, in *amusement+awe*, colorful balloons and a rainbow in mountain valley create a fantastical yet dignified visual language, while in *awe+fear*, the transformation of mountain contours shapes the rock formations into a devil-like face, collectively reinforcing a sense of wonder and fear. When fusing emotions, we are essentially organically integrating emotional semantics at visual level, allowing CoEmoGen not only to generate single-emotion images but also to explore more multi-dimensional emotional experiences.

Conclusion and Future Work

In this paper, we develop CoEmoGen, a novel EICG pipeline excelling in semantic coherence and high scalability. Leveraging MLLMs, we obtain reliable context-rich sentence-level captions for the images in EmoSet to serve as semantically-coherent guidance. Referring to psychological theory, we design a HiLoRA module, including polarity-shared LoRAs to model common low-level features and emotion-specific LoRAs to capture high-level exclusive semantics. We demonstrate the superiority of the proposed CoEmoGen in EICG from qualitative, quantitative, and user study perspectives, and further collect and construct the first large-scale emotional art image dataset, EmoArt, to concretely showcase high scalability. In future work, we plan to investigate the denoising process in depth, explicitly analyzing the dynamic shifts of attention toward emotion-related attributes across different denoising stages.

References

Bai, Z.; Wang, P.; Xiao, T.; He, T.; Han, Z.; Zhang, Z.; and Shou, M. Z. 2024. Hallucination of multimodal large language models: A survey. *arXiv preprint arXiv:2404.18930*.

- Betker, J.; Goh, G.; Jing, L.; Brooks, T.; Wang, J.; Li, L.; Ouyang, L.; Zhuang, J.; Lee, J.; Guo, Y.; et al. 2023. Improving image generation with better captions. *Computer Science*. <https://cdn.openai.com/papers/dall-e-3.pdf>, 2(3): 8.
- Borth, D.; Ji, R.; Chen, T.; Breuel, T.; and Chang, S.-F. 2013. Large-scale visual sentiment ontology and detectors using adjective noun pairs. In *Proceedings of the 21st ACM international conference on Multimedia*, 223–232.
- Brosch, T.; Pourtois, G.; and Sander, D. 2010. The perception and categorisation of emotional stimuli: A review. *Cognition and emotion*, 24(3): 377–400.
- Chen, T.; Xiong, W.; Zheng, H.; and Luo, J. 2020. Image sentiment transfer. In *Proceedings of the 28th ACM International Conference on Multimedia*, 4407–4415.
- Chen, W.; Xiao, H.; Zhang, E.; Hu, L.; Wang, L.; Liu, M.; and Chen, C. 2024. Sato: Stable text-to-motion framework. In *Proceedings of the 32nd ACM International Conference on Multimedia*, 6989–6997.
- Chen, W.; Yu, K.; Jia, H.; Yuan, K.; Tian, B.; Lai, S.; Xiao, H.; Zhang, E.; Wang, L.; and Yue, Y. 2025. ANT: Adaptive Neural Temporal-Aware Text-to-Motion Model. *arXiv preprint arXiv:2506.02452*.
- Dhariwal, P.; and Nichol, A. 2021. Diffusion models beat gans on image synthesis. *Advances in neural information processing systems*, 34: 8780–8794.
- Gal, R.; Alaluf, Y.; Atzmon, Y.; Patashnik, O.; Bermano, A. H.; Chechik, G.; and Cohen-Or, D. 2022. An image is worth one word: Personalizing text-to-image generation using textual inversion. *arXiv preprint arXiv:2208.01618*.
- Heusel, M.; Ramsauer, H.; Unterthiner, T.; Nessler, B.; and Hochreiter, S. 2017. Gans trained by a two time-scale update rule converge to a local nash equilibrium. *Advances in neural information processing systems*, 30.
- Ho, J.; Jain, A.; and Abbeel, P. 2020. Denoising diffusion probabilistic models. *Advances in neural information processing systems*, 33: 6840–6851.
- Ho, J.; and Salimans, T. 2022. Classifier-free diffusion guidance. *arXiv preprint arXiv:2207.12598*.
- Hu, E. J.; Shen, Y.; Wallis, P.; Allen-Zhu, Z.; Li, Y.; Wang, S.; Wang, L.; Chen, W.; et al. 2022. Lora: Low-rank adaptation of large language models. *ICLR*, 1(2): 3.
- Hu, Z.; Yuan, K.; Liu, X.; Yu, Z.; Zong, Y.; Shi, J.; Yue, H.; and Yang, J. 2025. Feallm: Advancing facial emotion analysis in multimodal large language models with emotional synergy and reasoning. *arXiv preprint arXiv:2505.13419*.
- Kim, J. M.; Bader, J.; Alaniz, S.; Schmid, C.; and Akata, Z. 2024. Datadream: Few-shot guided dataset generation. In *European Conference on Computer Vision*, 252–268. Springer.
- Kumari, N.; Zhang, B.; Zhang, R.; Shechtman, E.; and Zhu, J.-Y. 2023. Multi-concept customization of text-to-image diffusion. In *Proceedings of the IEEE/CVF conference on computer vision and pattern recognition*, 1931–1941.
- Kuznetsova, A.; Rom, H.; Alldrin, N.; Uijlings, J.; Krasin, I.; Pont-Tuset, J.; Kamali, S.; Popov, S.; Mallocci, M.; Kolesnikov, A.; et al. 2020. The open images dataset v4: Unified image classification, object detection, and visual relationship detection at scale. *International journal of computer vision*, 128(7): 1956–1981.
- Li, Y.; Lai, Z.; Bao, W.; Tan, Z.; Dao, A.; Sui, K.; Shen, J.; Liu, D.; Liu, H.; and Kong, Y. 2025. Visual Large Language Models for Generalized and Specialized Applications. *arXiv preprint arXiv:2501.02765*.
- Liu, D.; Jiang, Y.; Pei, M.; and Liu, S. 2018. Emotional image color transfer via deep learning. *Pattern Recognition Letters*, 110: 16–22.
- Liu, X.; Yuan, K.; Niu, X.; Shi, J.; Yu, Z.; Yue, H.; and Yang, J. 2024a. Multi-scale promoted self-adjusting correlation learning for facial action unit detection. *IEEE Transactions on Affective Computing*.
- Liu, X.; Zhang, Y.; Yu, Z.; Lu, H.; Yue, H.; and Yang, J. 2024b. rppg-mae: Self-supervised pretraining with masked autoencoders for remote physiological measurements. *IEEE Transactions on Multimedia*, 26: 7278–7293.
- Loshchilov, I.; and Hutter, F. 2017. Decoupled weight decay regularization. *arXiv preprint arXiv:1711.05101*.
- Lu, H.; Niu, X.; Wang, J.; Wang, Y.; Hu, Q.; Tang, J.; Zhang, Y.; Yuan, K.; Huang, B.; Yu, Z.; et al. 2024. Gpt as psychologist? preliminary evaluations for gpt-4v on visual affective computing. In *Proceedings of the IEEE/CVF Conference on Computer Vision and Pattern Recognition*, 322–331.
- Machajdik, J.; and Hanbury, A. 2010. Affective image classification using features inspired by psychology and art theory. In *Proceedings of the 18th ACM international conference on Multimedia*, 83–92.
- Mikels, J. A.; Fredrickson, B. L.; Larkin, G. R.; Lindberg, C. M.; Maglio, S. J.; and Reuter-Lorenz, P. A. 2005. Emotional category data on images from the International Affective Picture System. *Behavior research methods*, 37: 626–630.
- Minsky, M. 2007. *The emotion machine: Commonsense thinking, artificial intelligence, and the future of the human mind*. Simon and Schuster.
- Nichol, A.; Dhariwal, P.; Ramesh, A.; Shyam, P.; Mishkin, P.; McGrew, B.; Sutskever, I.; and Chen, M. 2021. Glide: Towards photorealistic image generation and editing with text-guided diffusion models. *arXiv preprint arXiv:2112.10741*.
- Paszke, A.; Gross, S.; Massa, F.; Lerer, A.; Bradbury, J.; Chanan, G.; Killeen, T.; Lin, Z.; Gimelshein, N.; Antiga, L.; et al. 2019. Pytorch: An imperative style, high-performance deep learning library. *Advances in neural information processing systems*, 32.
- Pearce, M. T.; Zaidel, D. W.; Vartanian, O.; Skov, M.; Leder, H.; Chatterjee, A.; and Nadal, M. 2016. Neuroaesthetics: The cognitive neuroscience of aesthetic experience. *Perspectives on psychological science*, 11(2): 265–279.
- Peebles, W.; and Xie, S. 2023. Scalable diffusion models with transformers. In *Proceedings of the IEEE/CVF international conference on computer vision*, 4195–4205.
- Peng, K.-C.; Chen, T.; Sadovnik, A.; and Gallagher, A. C. 2015. A mixed bag of emotions: Model, predict, and transfer

- emotion distributions. In *Proceedings of the IEEE conference on computer vision and pattern recognition*, 860–868.
- Radford, A.; Kim, J. W.; Hallacy, C.; Ramesh, A.; Goh, G.; Agarwal, S.; Sastry, G.; Askell, A.; Mishkin, P.; Clark, J.; et al. 2021. Learning transferable visual models from natural language supervision. In *International conference on machine learning*, 8748–8763. PmLR.
- Rao, T.; Li, X.; and Xu, M. 2020. Learning multi-level deep representations for image emotion classification. *Neural processing letters*, 51: 2043–2061.
- Rombach, R.; Blattmann, A.; Lorenz, D.; Esser, P.; and Ommer, B. 2022. High-resolution image synthesis with latent diffusion models. In *Proceedings of the IEEE/CVF conference on computer vision and pattern recognition*, 10684–10695.
- Ruiz, N.; Li, Y.; Jampani, V.; Pritch, Y.; Rubinstein, M.; and Aberman, K. 2023. Dreambooth: Fine tuning text-to-image diffusion models for subject-driven generation. In *Proceedings of the IEEE/CVF conference on computer vision and pattern recognition*, 22500–22510.
- Saharia, C.; Chan, W.; Saxena, S.; Li, L.; Whang, J.; Denton, E. L.; Ghasemipour, K.; Gontijo Lopes, R.; Karagol Ayan, B.; Salimans, T.; et al. 2022. Photorealistic text-to-image diffusion models with deep language understanding. *Advances in neural information processing systems*, 35: 36479–36494.
- Song, J.; Meng, C.; and Ermon, S. 2020. Denoising diffusion implicit models. *arXiv preprint arXiv:2010.02502*.
- Sun, S.; Jia, J.; Wu, H.; Ye, Z.; and Xing, J. 2023. Msnet: A deep architecture using multi-sentiment semantics for sentiment-aware image style transfer. In *ICASSP 2023-2023 IEEE international conference on acoustics, speech and signal processing (ICASSP)*, 1–5. IEEE.
- Tao, J.; and Tan, T. 2005. Affective computing: A review. In *International Conference on Affective computing and intelligent interaction*, 981–995. Springer.
- Tian, K.; Jiang, Y.; Yuan, Z.; Peng, B.; and Wang, L. 2025. Visual autoregressive modeling: Scalable image generation via next-scale prediction. *Advances in neural information processing systems*, 37: 84839–84865.
- Wang, X.; Jia, J.; and Cai, L. 2013. Affective image adjustment with a single word. *The Visual Computer*, 29: 1121–1133.
- Weng, S.; Zhang, P.; Chang, Z.; Wang, X.; Li, S.; and Shi, B. 2023. Affective image filter: Reflecting emotions from text to images. In *Proceedings of the IEEE/CVF International Conference on Computer Vision*, 10810–10819.
- Wieser, M. J.; Klupp, E.; Weyers, P.; Pauli, P.; Weise, D.; Zeller, D.; Classen, J.; and Mühlberger, A. 2012. Reduced early visual emotion discrimination as an index of diminished emotion processing in Parkinson’s disease?—Evidence from event-related brain potentials. *Cortex*, 48(9): 1207–1217.
- Xing, B.; Yu, Z.; Liu, X.; Yuan, K.; Ye, Q.; Xie, W.; Yue, H.; Yang, J.; and Kälviäinen, H. 2024. Emo-llama: Enhancing facial emotion understanding with instruction tuning. *arXiv preprint arXiv:2408.11424*.
- Xing, B.; Yuan, K.; Yu, Z.; Liu, X.; and Kälviäinen, H. 2025. AU-TTT: Vision Test-Time Training model for Facial Action Unit Detection. *arXiv preprint arXiv:2503.23450*.
- Yang, J.; Feng, J.; and Huang, H. 2024. EmoGen: Emotional image content generation with text-to-image diffusion models. In *Proceedings of the IEEE/CVF Conference on Computer Vision and Pattern Recognition*, 6358–6368.
- Yang, J.; Huang, Q.; Ding, T.; Lischinski, D.; Cohen-Or, D.; and Huang, H. 2023. Emoset: A large-scale visual emotion dataset with rich attributes. In *Proceedings of the IEEE/CVF International Conference on Computer Vision*, 20383–20394.
- Yang, J.; Li, J.; Wang, X.; Ding, Y.; and Gao, X. 2021. Stimuli-aware visual emotion analysis. *IEEE Transactions on Image Processing*, 30: 7432–7445.
- Yang, J.; She, D.; Sun, M.; Cheng, M.-M.; Rosin, P. L.; and Wang, L. 2018. Visual sentiment prediction based on automatic discovery of affective regions. *IEEE Transactions on Multimedia*, 20(9): 2513–2525.
- Yuan, K.; Yu, Z.; Liu, X.; Xie, W.; Yue, H.; and Yang, J. 2024. Auformer: Vision transformers are parameter-efficient facial action unit detectors. In *European Conference on Computer Vision*, 427–445. Springer.
- Zhang, L.; Rao, A.; and Agrawala, M. 2023. Adding conditional control to text-to-image diffusion models. In *Proceedings of the IEEE/CVF international conference on computer vision*, 3836–3847.
- Zhang, R.; Isola, P.; Efros, A. A.; Shechtman, E.; and Wang, O. 2018. The unreasonable effectiveness of deep features as a perceptual metric. In *Proceedings of the IEEE conference on computer vision and pattern recognition*, 586–595.
- Zhang, Y.; Lu, H.; Hu, Q.; Wang, Y.; Yuan, K.; Liu, X.; and Wu, K. 2025a. Period-LLM: Extending the Periodic Capability of Multimodal Large Language Model. In *Proceedings of the Computer Vision and Pattern Recognition Conference*, 29237–29247.
- Zhang, Y.; Lu, H.; Liu, X.; Chen, Y.; and Wu, K. 2025b. Advancing generalizable remote physiological measurement through the integration of explicit and implicit prior knowledge. *IEEE Transactions on Image Processing*.
- Zhang, Y.; Yuan, K.; Lu, H.; Yue, Y.; Chen, J.; and Wu, K. 2025c. MedTVT-R1: A Multimodal LLM Empowering Medical Reasoning and Diagnosis. *arXiv preprint arXiv:2506.18512*.
- Zhao, S.; Yao, X.; Yang, J.; Jia, G.; Ding, G.; Chua, T.-S.; Schuller, B. W.; and Keutzer, K. 2021. Affective image content analysis: Two decades review and new perspectives. *IEEE Transactions on Pattern Analysis and Machine Intelligence*, 44(10): 6729–6751.
- Zhou, B.; Lapedriza, A.; Khosla, A.; Oliva, A.; and Torralba, A. 2017. Places: A 10 million image database for scene recognition. *IEEE transactions on pattern analysis and machine intelligence*, 40(6): 1452–1464.
- Zhu, C.; Li, K.; Ma, Y.; He, C.; and Li, X. 2024. Multiboost: Towards generating all your concepts in an image from text. *arXiv preprint arXiv:2404.14239*.